HHS Public Access

Author manuscript

Acta Biomater. Author manuscript; available in PMC 2016 January 31.

Published in final edited form as:

Acta Biomater. 2014 February ; 10(2): 623–629. doi:10.1016/j.actbio.2013.10.021.

Biological magnetic cellular spheroids as building blocks for tissue engineering

Brandon Mattix[a], **Timothy R. Olsen**[a], **Yu Gu**[b], **Megan Casco**[a], **Austin Herbst**[a], **Dan T. Simionescu**[a], **Richard P. Visconti**[c], **Konstantin G. Kornev**[b], and **Frank Alexis**[a,d,*]

[a]Department of Bioengineering, Clemson University, 301 Rhodes Research Center, Clemson, SC 29634, USA

[b]Department of Materials Science and Engineering, Clemson University, 161 Sirrine Hall, Clemson, SC 29634, USA

[c]Department of Regenerative Medicine and Cell Biology, Medical University of South Carolina, 173 Ashley Avenue, BSB 601, Charleston, SC 29425, USA

[d]Institute of Biological Interfaces of Engineering, 401-2 Rhodes Engineering Research Center, Clemson, SC 29634, USA

Abstract

Magnetic nanoparticles (MNPs), primarily iron oxide nanoparticles, have been incorporated into cellular spheroids to allow for magnetic manipulation into desired shapes, patterns and 3-D tissue constructs using magnetic forces. However, the direct and long-term interaction of iron oxide nanoparticles with cells and biological systems can induce adverse effects on cell viability, phenotype and function, and remain a critical concern. Here we report the preparation of biological magnetic cellular spheroids containing magnetoferritin, a biological MNP, capable of serving as a biological alternative to iron oxide magnetic cellular spheroids as tissue engineered building blocks. Magnetoferritin NPs were incorporated into 3-D cellular spheroids with no adverse effects on cell viability up to 1 week. Additionally, cellular spheroids containing magnetoferritin NPs were magnetically patterned and fused into a tissue ring to demonstrate its potential for tissue engineering applications. These results present a biological approach that can serve as an alternative to the commonly used iron oxide magnetic cellular spheroids, which often require complex surface modifications of iron oxide NPs to reduce the adverse effects on cells.

Keywords

Magnetic nanoparticles; Ferritin; Magnetoferritin; Tissue engineering

*Corresponding author at: Department of Bioengineering, Clemson University, 301 Rhodes Research Center, Clemson, SC 29634, USA. Tel.: +1 864 656 5003; fax: +1 864 656 4466. falexis@clemson.edu (F. Alexis).

Appendix A. Supplementary data

Supplementary data associated with this article can be found, in the online version, at http://dx.doi.org/10.1016/j.actbio.2013.10.021.

Appendix B. Figures with essential color discrimination

Certain figures in this article, particularly Figs. 1–4, are difficult to interpret in black and white. The full colour images can be found in the on-line version, at http://dx.doi.org/10.1016/j.actbio.2013.10.021).

1. Introduction

A variety of nanoparticles (NPs), including magnetic iron oxide NPs, gold NPs, carbon nanotubes and polymeric NPs, have been integrated with tissue engineering to provide in situ imaging, drug delivery, mechanical properties and functionality [1,2]. Nanotechnology can benefit tissue engineering due to its ability to control interactions at sub-cellular levels that are not possible using common tissue engineering techniques [3–5]. In particular, magnetic nanoparticles (MNPs) have been integrated with tissue engineering applications for tissue patterning and maturation [6–9]. However, the direct and long-term interaction of MNPs with cells can induce adverse effects on cell viability, phenotype and function, and therefore remain a critical concern [6,10–13]. Commonly investigated MNPs include ferrites (cobalt [14], manganese [15], nickel [16]), manganites, as well as metals (Fe [17], Co, Ni [18]) and their alloys. However, before these ferrite NPs may be used, their surfaces must be modified with polymers [19–21], oleates [22,23], dextran [24,25], gold or silica [26] to improve the MNPs' biocompatibility. Because of the complex chemistry inherent in such modifications, there is a critical need to investigate biological MNPs as an alternative to the commonly used iron oxide MNPs to effectively reduce adverse effects on cells, thereby allowing for long-term use in tissue engineering applications.

Magnetoferritin is a potential biological MNP that can address the adverse cellular effects of common metallic MNPs. Compared to other surface-modified iron oxide MNPs, the apoferritin shell of magnetoferritin is protein based, unlike other inorganic coatings, thereby making it a naturally biocompatible surface coating. The primary role of ferritin, a natural protein in the body, is short- and long-term iron storage. The intracellular functions of ferritin include providing iron reserves for cytochromes, hemoglobin, myoglobin and nitrogenase [27], with normal blood serum levels ranging from 10 to 200 ng ml^{-1}, and mean values of 103 and 35.6 ng ml^{-1} for males and females, respectively [28]. Furthermore, apoferritin demonstrates ferroxidase activity by catalyzing the oxidation of Fe(II), an initial step in the preparation of iron for storage in ferritin [29,30]. In this work, we hypothesized that a biological magnetic NP will be a less toxic alternative than iron oxide MNPs when integrated into cellular spheroids. Specifically, we prepared magnetoferritin NPs with tailored loading and magnetic properties, analyzed its effects on cell viability, and demonstrated its ability to mediate tissue patterning via magnetic force assembly. The results demonstrate that magnetoferritin NPs have the potential to mitigate the cytotoxicity that currently prevents prolonged use of MNPs in tissue engineering applications.

2. Materials and methods

2.1. Materials

Apoferritin (equine spleen), trimethylamine-n-oxide ($(CH_3)_3N(O)$, 98%), AMPSO ($C_7H_{17}NO_5S$, 99%), ammonium (II) sulfate hexahydrate ($(NH_4)_2Fe(SO_4)_2{\cdot}6H_2O$, 99%), potassium ferrocyanide ($K_4\ Fe(CN)_6{\cdot}3H_2O$, 98.5–102%) and phosphate-buffered saline (PBS) were supplied by Sigma-Aldrich. Hydrocholoric acid (6 N) was supplied by Ricca Chemical Company. PrestoBlue cell viability reagent, LIVE/DEAD cell viability kit, collagense (type IV) and bovine collagen type I were supplied by Life Technologies. Commercial iron oxide MNPs were supplied by SkySpring Nanomaterials, Inc. (Fe_3O_4, 20–

30 nm). Trypsin (0.25%) was supplied by Thermo Scientific. Zinc-buffered formalin (Z-fix) was supplied by Anatech Ltd.

2.2. Magnetoferritin synthesis

Magnetoferritin NPs were synthesized by gradually loading apoferritin with iron oxide NPs [31]. Apoferritin (0.44 M) was placed in an AMPSO buffer solution (50 mM, pH 8.6) and heated to 65 °C. Aliquots of ferrous ammonium sulfate (Fe^{2+}, 0.1 M) and triemethylamine-N-oxide (Me_3NO, 0.07 M) were added dropwise to the reaction solution. Each addition of Fe(II) (0.612 μmol) was followed by a stoichiometric aliquot of Me_3NO (3 Fe(II):2 Me_3NO, 0.612 μmol:0.41 μmol) and left for 15 min before repeating the stepwise addition. One synthesis cycle was defined as one sequential addition of Fe^{2+} and Me_3NO. Samples were dialyzed in water at 4 °C for 2 days prior to use (MWCO: 12–14 kDa).

2.3. Magnetoferritin characterization

A bichinchoninic acid (BCA, Lambda Biotech, Inc.) assay was performed to quantify the amount of protein. The iron content within magnetoferritin NPs was quantified using an established technique to quantify iron content in solutions [32]. Briefly, magnetoferritin NPs were first dissociated using 5 N HCl for 72 h, followed by quantification of free iron within solutions using a Perls' Prussian blue colorimetric technique. Dissociated samples were incubated with 5% potassium ferrocyanide for 15 min, followed by absorbance readings at 562 nm. Additionally, magnetoferritin NPs were characterized using scanning transmission electron microscopy (STEM) and energy-dispersive spectrometry (EDS) on a Hitachi 2000 scanning transmission electron microscope. The magnetic properties of magnetoferritin NPs were characterized using an alternating gradient magnetometer (AGM 2900, Princeton Measurements Inc.).

2.4. Cell culture

Primary rat aortic smooth muscle cells (SMCs) were used for all cellular spheroid studies. Cells were cultured in monolayer cultures using Dulbeco's modified Eagle's medium:F-12 (ATCC, 1:1) supplemented with 10% fetal bovine serum (Atlanta Biologics) and 1% penicillin–streptomycin–amphotericin (MediaTech, Inc.) at 37 °C and 5% of CO_2.

2.5. Cellular spheroid assembly

Equal volumes of solutions containing NPs (magnetoferritin NPs or iron oxide MNPs), collagen and SMCs in medium were combined and immediately dispensed using the hanging drop method. Samples were inverted and incubated at 37 °C with 5% CO_2 for 3 days prior to use to allow for spheroid assembly. Cellular spheroids were assembled using 20,000 cells per spheroid. Collagen was incorporated into cellular spheroids at different concentrations, depending on the application (17 μg ml^{-1} for viability; 5 μg ml^{-1} for magnetic patterning).

To assemble uptake MNP spheroids, a monolayer cell culture flask (~90% confluence) was incubated with MNP-containing cell culture medium for 24 h. The bottoms of culture flasks were covered with square magnets (K&J Magnetics, Inc., 12.7 × 12.7 mm, 1.6 mm thick, vendor calculated pull force = 3.59 lbs) to promote MNP internalization into cells. Media

solutions containing iron oxide MNPs were sonicated prior to addition to cells. After incubation, cells were washed five times to remove free MNPs, trypsinized, collected, placed on a magnetic wash tool and allowed to sit for 5 min. The supernatant was discarded and the remaining magnetically attracted cells were suspended in fresh medium. Solutions of magnetically attracted cells and collagen were combined and dispensed using the hanging drop method, as mentioned previously. Collagen was prepared according to the manufacturer's recommendations and kept on ice prior to use for all samples.

2.6. Quantification of NP uptake

Magnetic cellular spheroids were fabricated with magnetoferritin NPs (500 μg ml^{-1}, 7.5 μg per spheroid, 0.375 ng per cell). Spheroids (n = 10, dispersed and uptake) were dissociated via incubation with collagenase for 80 min at 37 °C, followed by incubation with trypsin for 10 min at 37 °C. Spheroids were then centrifuged and physically dissociated in 1 ml of medium. Next, samples were placed on a magnetic wash tool for 5 min. The supernatant was collected and the remaining cells (magnetically attracted) suspended in 1 ml of fresh medium. The amounts of cells in the supernatant and magnet solution were quantified using a hemocytometer. Spheroids were collected and analyzed after 3 days of assembly in a hanging drop. Three separate batches of spheroids were used for analysis.

2.7. Cellular spheroid viability

Magnetic cellular spheroids were fabricated with magnetoferritin NPs (500 μg ml^{-1}) or iron oxide MNPs (300 μg ml^{-1}) and compared to control cellular spheroids without MNPs. Spheroids were first dissociated with collagenase (80 min) and trypsin (10 min) as previously described, and allowed to adhere to a tissue-treated well plate overnight. A PrestoBlue cell viability assay was performed to quantify cell viability compared to MNP-free controls after spheroid dissociation (at least three repeats per sample). Magnetic cellular spheroids assembled using iron oxide MNPs had a lower MNP concentration than magnetoferritin NPs due to MNP concentrations used in magnetic patterning studies.

To qualitatively assess the viability of intact spheroids, simultaneous LIVE/DEAD confocal microscopy was performed. Spheroids were washed with sterile PBS and incubated with LIVE/DEAD working solution, prepared according to the manufacturer's protocol, containing calcein AM (live, green) and ethidium homodimer-1 (EthD-1, dead, red). After staining, spheroids were washed with PBS and fixed in Z-fix for 30 min. Samples were then imaged using a Nikon Eclipse Ti confocal microscope. All spheroids were collected and analyzed after 3 days of assembly in a hanging drop.

Additionally, dissociated spheroids were quantitatively analyzed using a LIVE/DEAD viability kit. Spheroid viability was quantified using a Tali Image-Based Cytometer (Life Technologies, Green + Red System Protocol). For each sample, 10 spheroids were dissociated as previously described with collagenase and trypsin. Cell solutions were analyzed for viability per manufacturer specifications using calcein AM (live) and EthD-1 (dead). Live and dead cells were quantified using the Tali Image-Based Cytometer. An unstained sample was first analyzed to set the background and to determine the fluorescent thresholds. Each sample was then gated according to these initial thresholds. All spheroids

were collected and analyzed after 3 days of assembly in a hanging drop. At least three samples per spheroid type were analyzed.

2.8. Histology

Magnetoferritin cellular spheroids were processed and sectioned via standard paraffin sectioning techniques. Samples were dehydrated using ethanol and xylene prior to being embedded in paraffin. Sections, 5 μm thick, were stained with hematoxylin and eosin and Lillie's technique for Turnbull's blue reaction (Poly Scientific).

2.9. Magnetic patterning

Commercial axially magnetized ring magnets (SuperMagnet-Man, 10 mm diameter), were secured to the bottom of glass chamber slides containing coverglass bottoms. Four hundred magnetic cellular spheroids (dispersed) were placed in the chamber and allowed to magnetically align. Tissue structures were allowed to fuse for 4 days prior to imaging. The magnet patterns were kept static throughout the 4 days and removed for imaging. Samples were imaged using a Nikon AZ100 multizoom microscope. Different concentrations of magnetoferritin NPs and iron oxide MNPs were used due to the magnetic attraction of cellular spheroids.

2.10. Statistical analysis

A two-tailed Student's *t*-test was used to assess the significance of cell viability studies compared to control cellular spheroids without MNPs. Statistical significance was set at $p < 0.05$. Error bars on graphs represent the standard deviation from the mean.

3. Results and discussion

3.1. Magnetoferritin synthesis and characterization

By varying the number of cycles (from 10 to 70) performed during magnetoferritin NP synthesis, we were able to tailor the loading of iron oxide into equine spleen apoferritin protein shells. By increasing the number of synthesis cycles, we increased the iron oxide loading per ferritin shell from 810 to 3395 (iron oxide per protein, Fig. 1a). While the maximum loading of iron per ferritin shell is 4500 [27,33], we have synthesized magnetoferritin NPs with maximum loadings of around 3400 – similar to other groups [31,33,34]. Additionally, by varying the iron oxide content within the magnetoferritin NPs, we were able to control the magnetic properties of these biological MNPs, as a higher loading content corresponded to stronger superparamagnetic properties with the application of an external magnetic field. In our subsequent analysis of our magnetic manipulation of magnetoferritin NPs, we determined that 70 cycle magnetoferritin NPs were capable of magnetic manipulation and attraction in contrast to unloaded apoferritin NPs (Fig. 1b). Magnetoferritin NPs synthesized using 70 cycles were chosen based on previous results that analyzed the loading (iron oxide per protein) of various synthesis cycles (Supplementary Fig. S1). Furthermore, the ability to tailor the magnetic properties of magnetoferritin NPs was confirmed by analyzing the magnetic hysteresis of magnetoferritin NPs compared to iron oxide MNPs (Fig. 1c and d). Unlike iron oxide MNPs, the magnetoferritin NPs are superparamagnetic, with almost zero remanence and coercivity. With increasing cycles, the

shape of the magnetization curve stays the same while the saturation magnetization increases, confirming an increase in magnetic properties in 70-cycle magnetoferritin NPs. Finally, magnetoferritin NPs were characterized using STEM and EDS (Fig. 2). Z-contrast was used for STEM imaging to differentiate the iron oxide cores from their protein shell. Results confirmed that magnetoferritin NPs contained iron oxide, as indicated by the presence of both iron (red) and oxygen (blue) compared to apoferritin controls in EDS analysis. We used EDS to quantitatively confirm the iron content from magnetoferritin formulations, as demonstrated by an atomic percent increase in iron for 10- and 70-cycle magnetoferritin NPs (12.6% and 29.5%, respectively) compared to unloaded apoferritin (0.52%). The small amount of iron present in apoferritin samples was likely due to residual iron from the unloading of the native ferritin NPs. By controlling the loading of iron oxide into apoferritin shells and therefore the magnetic properties of magnetoferritin NPs, we demonstrated the ability to prepare tailored biological magnetic NPs.

3.2. Incorporation of magnetoferritin into cellular spheroids

To determine the capacity for magnetoferritin NPs to serve as effective magnetic NPs for tissue engineering applications, magnetoferritin NPs were incorporated into cellular spheroids. Specifically, using rat aortic smooth muscle cells, magnetoferritin NPs (70 cycles) were incorporated into cellular spheroids using two techniques: uptake and dispersed (Fig. 3a). Uptake cellular spheroids refer to spheroids composed of cells that have internalized magnetoferritin NPs. Dispersed cellular spheroids refer to a method of spheroid synthesis in which magnetoferritin NPs are dispersed throughout the extracellular space. Histological analysis was performed to analyze the dispersion of magnetoferritin NPs within cellular spheroids (Fig. 3b). Samples were stained using hemotoxylin and eosin (H&E), and Lillie's Turnbull blue reaction to show the presence of iron oxide within magnetoferritin NPs (iron = black). Magnetoferritin was visible in both stains, appearing red-orange in H&E and black in Lillie's Turnbull blue reaction. The results confirmed the dispersion of magnetoferritin NPs throughout the cellular spheroids using both spheroid formulations (uptake and dispersed) at magnetoferritin concentrations of 82 μg ml^{-1}. Additionally, as the internalization of iron oxide MNPs into cells can induce cytotoxic effects, interaction between cells and MNPs should be minimized [13]. Compared to iron oxide MNPs, results showed that the percentage of cells internalizing magnetoferrtin NPs with dispersed cellular spheroids was significantly lower (14%) than that of iron oxide MNPs (28%) (Fig. 3c). These results indicate that magnetoferritin NPs can be effectively incorporated within magnetic cellular spheroids with reduced internalization into cells.

3.3. Effect of magnetoferritin on cellular spheroid viability

Next, studies were performed to determine if magnetoferritin NPs induced adverse effects on cell viability when integrated within cellular spheroids. Cell viability was analyzed using both qualitative (LIVE/DEAD fluorescent confocal microscopy) and quantitative analyses (PrestoBlue and LIVE/DEAD cytometry). All studies were performed using both types of magnetoferritin NP spheroids (uptake and dispersed) containing 500 μg ml^{-1} magnetoferritin and compared to spheroids containing iron oxide MNPs (300 μg ml^{-1}) and control spheroids with no MNPs. Using PrestoBlue, results showed that the presence of magnetoferritin NPs did not adversely affect cell viability compared to control spheroids

without MNPs at days 3 and 7 (Fig. 4a). However, spheroids containing iron oxide MNPs using both spheroid types showed decreased viability at both days 3 and 7 when compared to control spheroids without MNPs. Uptake and dispersed magnetoferritin NP spheroids demonstrated greater viability than control spheroids without MNPs at day 7. However, the decreased viability observed in the magnetoferritin uptake spheroids at day 3 could be due to the toxic effects of magnetoferritin particle uptake, and the higher viability observed in the day 7 magnetoferritin uptake spheroids is evidence of the survival or recovery of cells that did not die in response to initial magnetoferritin particle loading. These results suggest that the integration of biological nanomaterials with tissue engineering may not only overcome cytotoxicity from conventional nanomaterials, such as iron oxide MNPs, but could also promote cell growth. However, additional experiments must be performed to gain a full understanding of the effect of magnetoferritin NPs on cell proliferation and division. Next, samples were prepared to qualitatively analyze spheroid viability using LIVE/DEAD fluorescent confocal microscopy. Intact spheroids were imaged at day 3 to visualize live (green) and dead (red) cells throughout cellular spheroids (Fig. 4b). Confocal images showed that spheroids containing magnetoferritin NPs maintained high viability, as confirmed by limited expression of dead (red) cells throughout. However, spheroids containing iron oxide MNPs exhibited decreased viability compared to control spheroids without MNPs, as noted by an increased presence in dead cells throughout (red signal) compared to the spheroids without MNPs. The larger size of spheroids with magnetoferritin NPs can be attributed to the larger concentration of MNPs used (500 μg ml^{-1}) when compared to iron oxide MNP spheroids (300 μg ml^{-1}). Finally, dissociated samples were stained with a LIVE/DEAD kit and analyzed using a Tali Image-Based Cytometer to quantify cell viability. Results further confirmed that magnetoferritin NPs had no adverse effects on cell viability compared to MNP-free controls. In addition, spheroids containing iron oxide MNPs demonstrated decreased viability compared to controls. When normalized to control spheroids without MNPs, uptake and dispersed magnetoferritin NP spheroids had 83% and 96% cell viability, respectively, while uptake and dispersed iron oxide spheroids had 19% and 44% cell viability, respectively (Fig. 4c). Results obtained using both qualitative and quantitative analysis show that magnetoferritin NPs had no adverse effects on cell viability compared to MNP-free controls. Notably, spheroids composed of magnetoferritin NPs at a higher concentration (500 μg ml^{-1}) than iron oxide MNPs (300 μg ml^{-1}) maintained significantly higher cell viability up to 1 week. Using metallic iron oxide MNPs at concentrations of 50 μg ml^{-1}, Ho et al. [6] demonstrated noticeable toxicity in patterned cellular spheroids after only 48 h, thereby preventing potential use in tissue engineering applications that require long-term interaction with biological systems. Unlike iron oxide MNPs, magnetoferritin NPs are composed of a protein shell, which makes them more suitable for such applications. The presented results demonstrate that magnetoferritin NPs can serve as a more biocompatible alternative to iron oxide NPs by avoiding adverse effects related to MNP-induced cell toxicity.

3.4. Fabrication of fused tissue using magnetic force assembly

Finally, to demonstrate the application of magnetoferritin NPs for tissue engineering, fused tissue rings assembled using magnetic force assembly were used as a model. Results first confirmed the magnetic attraction of magnetoferritin cellular spheroids (Fig. 4d). Next,

using dispersed cellular spheroids, magnetoferritin NP spheroids (500 μg ml^{-1}) were magnetically patterned and fused over a 4 day period into a tissue ring (Fig. 4e). Samples were compared to magnetic cellular spheroids, with iron oxide MNPs as a control (300 μg ml^{-1}). Fusion was confirmed by the lack of individual cellular spheroids after 4 days of patterning, which formed a single homogeneous tissue void of gaps upon removal of the magnetic pattern. Although both rings were assembled using the same number of spheroids, magnetoferritin NP spheroids are assembled with a higher MNP content than iron oxide spheroids. Therefore, tissue rings assembled using magnetoferritin NPs are larger than those assembled using iron oxide MNPs due to differences in spheroid diameter between the two types of spheroids (magnetoferritin NPs and iron oxide MNPs). Based on these results, magnetoferritin can serve as a biological alternative to metallic MNPs for magnetic force assembly of tissues to promote tissue fusion.

4. Conclusions

We have demonstrated that NPs can safely be integrated with tissue engineering applications using magnetoferritin NPs and can serve as an alternative to iron oxide MNPs. The biological nature of magnetoferritin NPs has been shown to have the most potential in applications requiring long-term interaction with biological systems in that they exhibit no adverse effects on cell viability at concentrations much higher than that used with other metallic MNPs. In future research, we will expand upon our magnetoferritin NPs to fabricate complex 3-D tissue structures and multi-cellular tissues, and study the long-term biological response of cells, including the effects of magnetoferritin NPs on cell phenotype, proliferation and cell cycle.

Supplementary Material

Refer to Web version on PubMed Central for supplementary material.

Acknowledgments

This work was supported by a Beginning Grant-in-Aid-2BGIA11720004 award from the American Heart Association and an SC EPSCoR Grant for Exploratory Academic Research. The authors acknowledge the assistance of Dr. Terri Bruce, Mrs. Rhonda Powell and the Clemson Light Imaging Facility at Clemson University for technical support with the microscopy and viability studies, Mrs. Linda Jenkins for her assistance with histological techniques, and Dr. Joan Hudson and the Clemson Electron Microscope Facility staff for their assistance with imaging.

References

1. Shin SR, Jung SM, Zalabany M, Kim K, Zorlutuna P, Kim SB, et al. Carbonnanotube-embedded hydrogel sheets for engineering cardiac constructs and bioactuators. ACS Nano. 2013
2. Skardal A, Zhang J, McCoard L, Oottamasathien S, Prestwich GD. Dynamically crosslinked gold nanoparticle–hyaluronan hydrogels. Adv Mater. 2010; 22:4736–4740. [PubMed: 20730818]
3. Dvir T, Timko BP, Kohane DS, Langer R. Nanotechnological strategies for engineering complex tissues. Nat Nanotechnol. 2011; 6:13–22. [PubMed: 21151110]
4. Griffith LG, Naughton G. Tissue engineering – current challenges and expanding opportunities. Science. 2002; 295:1009–1014. [PubMed: 11834815]

5. Mironov V, Kasyanov V, Markwald RR. Nanotechnology in vascular tissue engineering: from nanoscaffolding towards rapid vessel biofabrication. Trends Biotechnol. 2008; 26:338–44. [PubMed: 18423666]
6. Ho VHB, Müller KH, Barcza A, Chen R, Slater NKH. Generation and manipulation of magnetic multicellular spheroids. Biomaterials. 2010; 31:3095–3102. [PubMed: 20045553]
7. Ino K, Ito A, Honda H. Cell patterning using magnetite nanoparticles and magnetic force. Biotechnol Bioeng. 2007; 97:1309–1317. [PubMed: 17216656]
8. Ino K, Okochi M, Honda H. Application of magnetic force-based cell patterning for controlling cell–cell interactions in angiogenesis. Biotechnol Bioeng. 2009; 102:882–890. [PubMed: 18821635]
9. Mack JJ, Corrin AA, dos Santos e Lucato SL, Dunn JCY, Wu BW, Cox BN. Enhanced cell viability via strain stimulus and fluid flow in magnetically actuated scaffolds. Biotechnol Bioeng. 2013; 110:936–946. [PubMed: 23042257]
10. Akiyama H, Ito A, Kawabe Y, Kamihira M. Cell-patterning using poly (ethylene glycol)-modified magnetite nanoparticles. J Biomed Mater Res Part A. 2010; 92A:1123–1130.
11. Bratt-Leal A, Kepple KL, Carpenedo RL, Cooke MT, McDevitt TC. Magnetic manipulation and spatial patterning of multi-cellular stem cell aggregates. Integr Biol. 2011
12. Ito A, Ino K, Kobayashi T, Honda H. The effect of RGD peptide-conjugated magnetite cationic liposomes on cell growth and cell sheet harvesting. Biomaterials. 2005; 26:6185–6193. [PubMed: 15899515]
13. Pislaru SV, Harbuzariu A, Agarwal G, Witt Aas Cvt Latg T, Gulati R, Sandhu NP, et al. Magnetic forces enable rapid endothelialization of synthetic vascular grafts. Circulation. 2006; 114:314–318.
14. Amiri S, Shokrollahi H. The role of cobalt ferrite magnetic nanoparticles in medical science. Mater Sci Eng C. 2013; 33:1–8.
15. Lu J, Ma S, Sun J, Xia C, Liu C, Wang Z, et al. Manganese ferrite nanoparticle micellar nanocomposites as MRI contrast agent for liver imaging. Biomaterials. 2009; 30:2919–2928. [PubMed: 19230966]
16. Rana S, Gallo A, Srivastava RS, Misra RDK. On the suitability of nanocrystalline ferrites as a magnetic carrier for drug delivery: functionalization, conjugation and drug release kinetics. Acta Biomater. 2007; 3:233–242. [PubMed: 17224313]
17. Park SJ, Kim S, Lee S, Khim ZG, Char K, Hyeon T. Synthesis and magnetic studies of uniform iron nanorods and nanospheres. J Am Chem Soc. 2000; 122:8581–8582.
18. Sun X, Gutierrez A, Yacaman MJ, Dong X, Jin S. Investigations on magnetic properties and structure for carbon encapsulated nanoparticles of Fe Co, Ni. Mater Sci Eng A. 2000; 286:157–160.
19. Yu M, Huang S, Yu KJ, Clyne AM. Dextran and polymer polyethylene glycol (PEG) coating reduce both 5 and 30 nm iron oxide nanoparticle cytotoxicity in 2D and 3D cell culture. Int J Mol Sci. 2012; 13:5554–5570. [PubMed: 22754315]
20. Huang H, Xie Q, Kang M, Zhang B, Zhang H, Chen J, et al. Labeling transplanted mice islet with polyvinylpyrrolidone coated superparamagnetic iron oxide nanoparticles for in vivo detection by magnetic resonance imaging. Nanotechnology. 2009; 20:365101. [PubMed: 19687538]
21. Lee H, Lee E, Do Kyung K, Jang NK, Jeong YY, Jon S. Antibiofouling polymer-coated superparamagnetic iron oxide nanoparticles as potential magnetic resonance contrast agents for in vivo cancer imaging. JACS. 2006; 128:7383–7389.
22. Chorny M, Alferiev IS, Fishbein I, Tengood JE, Folchman-Wagner Z, Forbes SP, et al. Formulation and in vitro characterization of composite biodegradable magnetic nanoparticles for magnetically guided cell delivery. Pharm Res. 2012; 29:1232–1241. [PubMed: 22274555]
23. Chorny M, Polyak B, Alferiev IS, Walsh K, Friedman G, Levy RJ. Magnetically driven plasmid DNA delivery with biodegradable polymeric nanoparticles. FASEB J. 2007; 21:2510–2519. [PubMed: 17403937]
24. Sharma R, Saini S, Ros PR, Hahn PF, Small WC, de Lange EE, et al. Safety profile of ultrasmall superparamagnetic iron oxide ferumoxtran-10: phase II clinical trial data. J Magn Reson Imaging. 1999; 9:291–294. [PubMed: 10077027]

25. Tassa C, Shaw SY, Weissleder R. Dextran-coated iron oxide nanoparticles: a versatile platform for targeted molecular imaging, molecular diagnostics, and therapy. Acc Chem Res. 2011; 44:842–852. [PubMed: 21661727]
26. Kim T, Momin E, Choi J, Yuan K, Zaidi H, Kim J, et al. Mesoporous silica-coated hollow manganese oxide nanoparticles as positive T1 contrast agents for labeling and MRI tracking of adipose-derived mesenchymal stem cells. JACS. 2011; 133:2955.
27. Theil EC. Ferritin: structure, gene regulation, and cellular function in animals, plants, and microorganisms. Annu Rev Biochem. 1987; 56:289–315. [PubMed: 3304136]
28. Walters GO, Miller FM, Worwood M. Serum ferritin concentration and iron stores in normal subjects. J Clin Pathol. 1973; 26:770–772. [PubMed: 4750458]
29. Bakker GR, Boyer RF. Iron incorporation into apoferritin. The role of apoferritin as a ferroxidase. J Biol Chem. 1986; 261:13182–13185. [PubMed: 3759957]
30. Sun S, Arosio P, Levi S, Chasteen ND. Ferroxidase kinetics of human liver apoferritin, recombinant H-chain apoferritin, and site-directed mutants. Biochemistry. 1993; 32:9362–9369. [PubMed: 8369307]
31. Wong KKW, Douglas T, Gider S, Awschalom DD, Mann S. Biomimetic synthesis and characterization of magnetic proteins (magnetoferritin). Chem Mater. 1998; 10:279–285.
32. Boutry S, Forge D, Burtea C, Mahieu I, Murariu O, Laurent S, et al. How to quantify iron in an aqueous or biological matrix: a technical note. Contrast Media Mol Imaging. 2009; 4:299–304. [PubMed: 19998319]
33. Martinez-Perez MJ, de Miguel R, Carbonera C, Martinez-Julvez M, Lostao A, Piquer C, et al. Size-dependent properties of magnetoferritin. Nanotechnology. 2010; 21:465707. [PubMed: 20975213]
34. Mitróová Z, Melníková L, Kováč J, Timko M, Kopčanský P. Synthesis and characterization of magnetoferritin. Acta Phys Pol A. 2012; 121:1318.

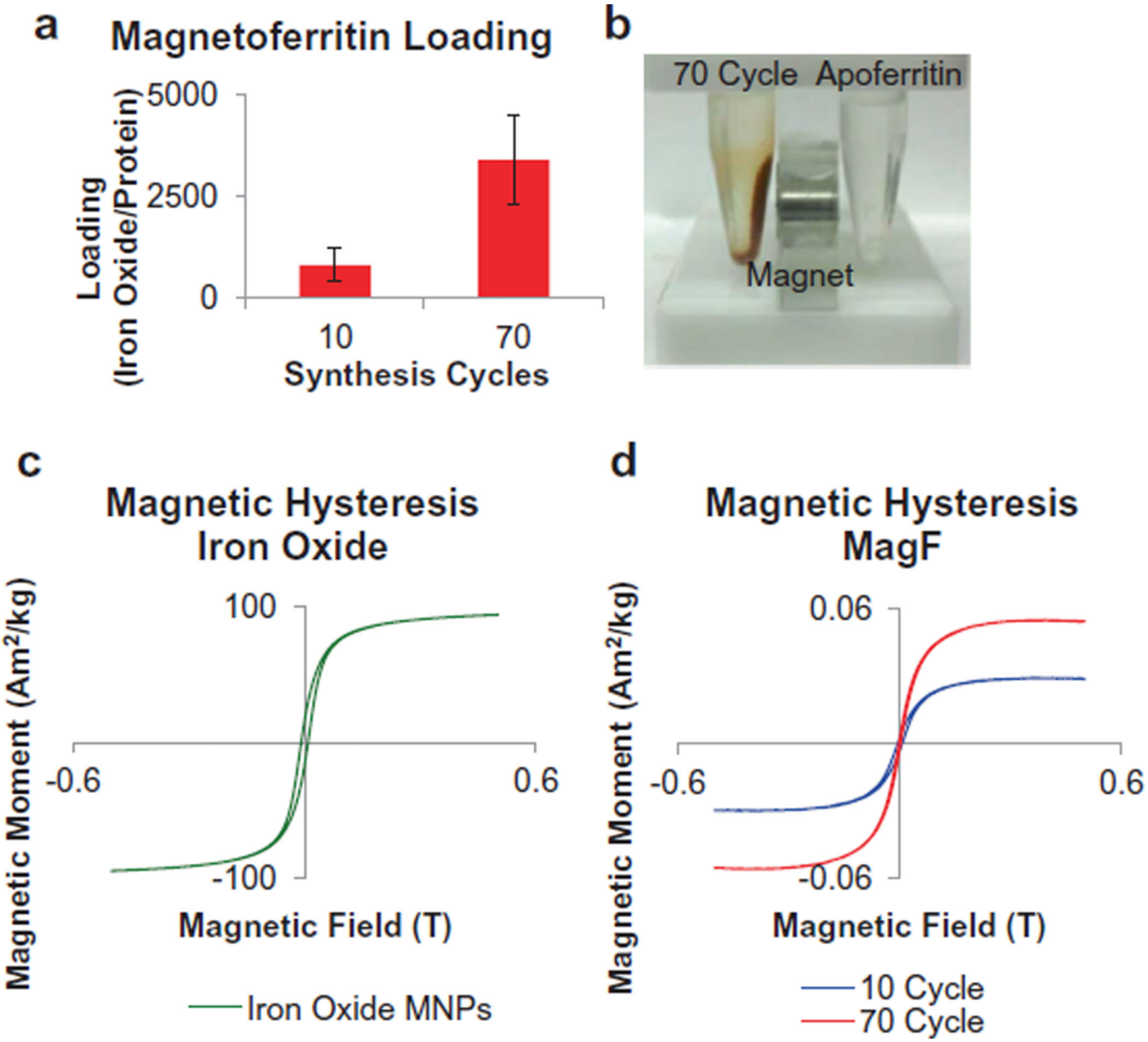

Fig. 1.

Characterization of magnetoferritin NPs. (a and b) The loading of iron oxide into magnetoferritin NPs was successfully controlled and resulted in magnetic NPs (70 cycle, compared to unloaded apoferritin protein NPs). Results confirmed control over loading content into magnetoferritin NPs based on the reaction cycles performed. (c and d) The ability to tailor magnetic properties of magnetoferritin NPs was confirmed by analyzing the magnetic hysteresis of samples. Results confirm that magnetoferritin NPs are superparamagnetic, and that magnetic properties can be enhanced by increasing the number of synthesis cycles performed.

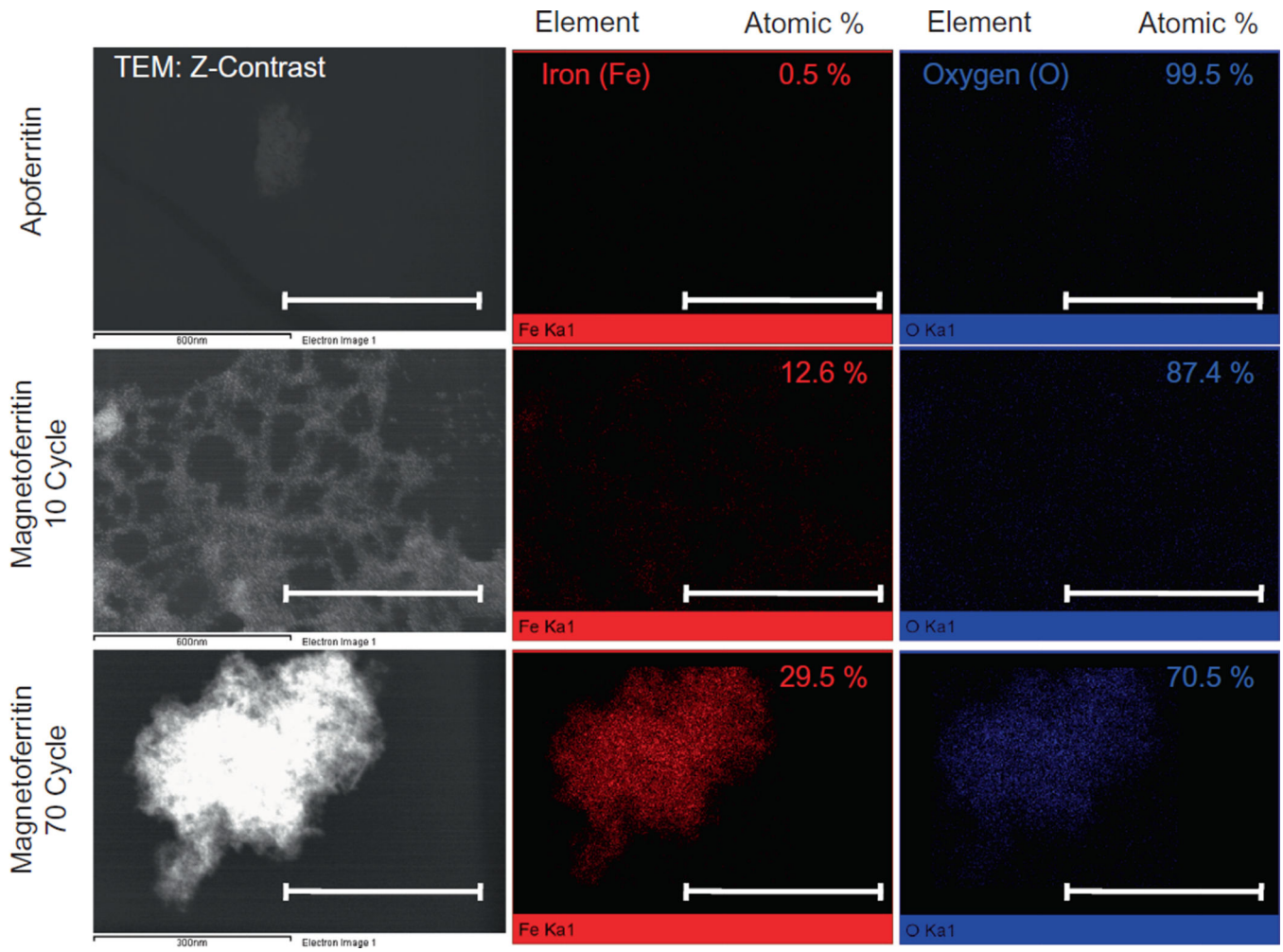

Fig. 2.

TEM and EDS characterization of magnetoferritin NPs. Magnetoferritin NPs were analyzed using STEM and EDS to confirm the presence of an iron oxide core, as noted by the high expressions of iron and oxygen in magnetoferritin NPs compared to in apoferritin protein shells. Magnetoferritin NPs were characterized by an atomic weight percent increase in iron between 10 (12.6%) and 70 cycle (29.5%) magnetoferritin NPs, confirming an increased presence of iron oxide. Scale bars: apoferritin, 10 cycle = 600 nm, 70 cycle = 300 nm.

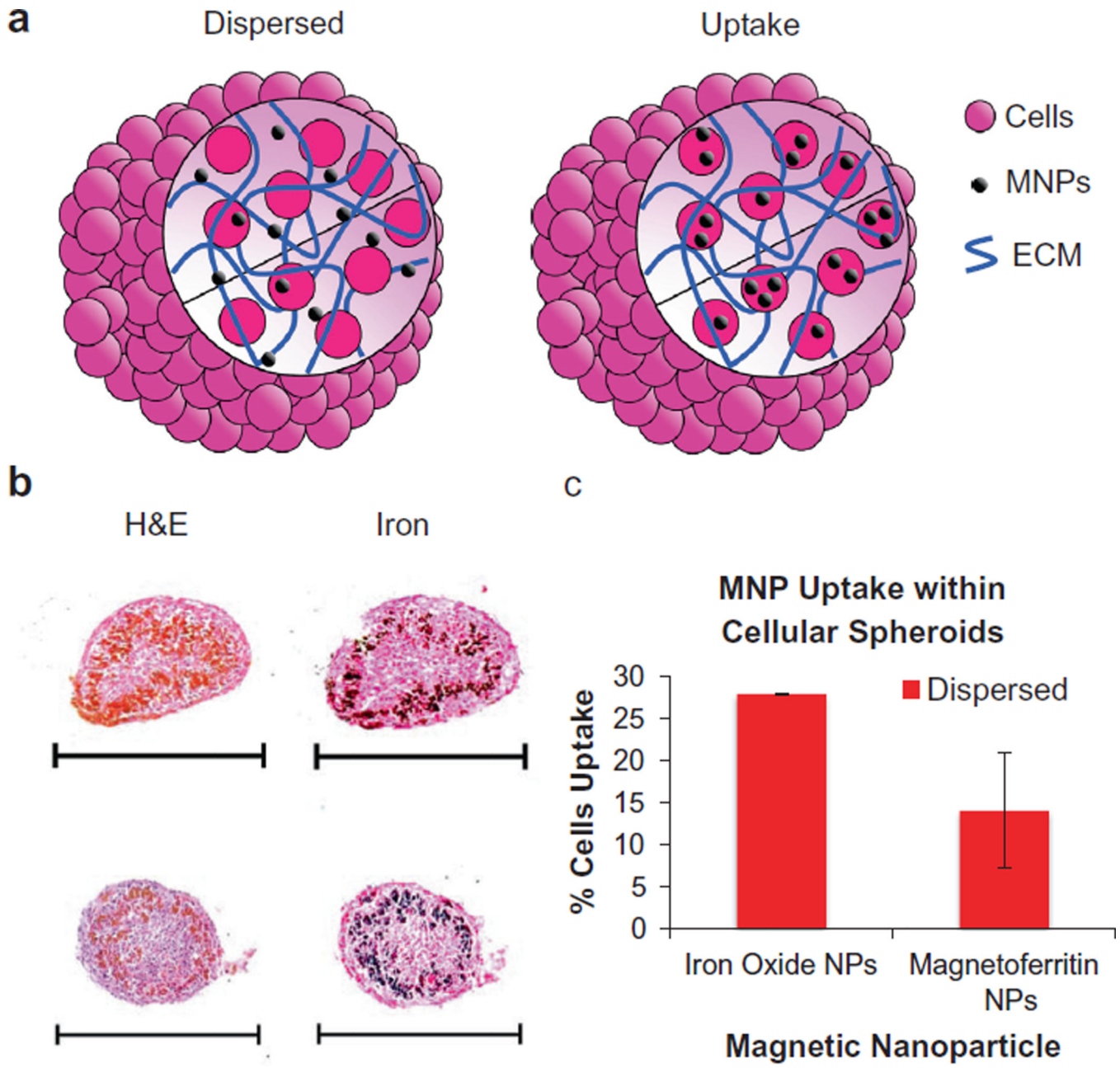

Fig. 3.

Magnetoferritin NPs in magnetic cellular spheroids. (a) Magnetoferritin NPs were incorporated into cellular spheroids using two methods: uptake and dispersed. Uptake spheroids contain cells (pink) that have internalized magnetoferritin NPs (black), while dispersed spheroids contain magnetoferritin NPs spatially distributed throughout the extracellular space. (b) Histological examination confirmed the assembly of cellular spheroids using both methods. Samples were stained with H&E and Lillie's technique for Turnbull's blue reaction (iron) to visualize the location of magnetoferritin NPs (scale bar = 500 μm). (c) Using dispersed cellular spheroids, results showed that magnetoferritin NPs resulted in lower cell uptake compared to iron oxide MNPs (*$p < 0.05$).

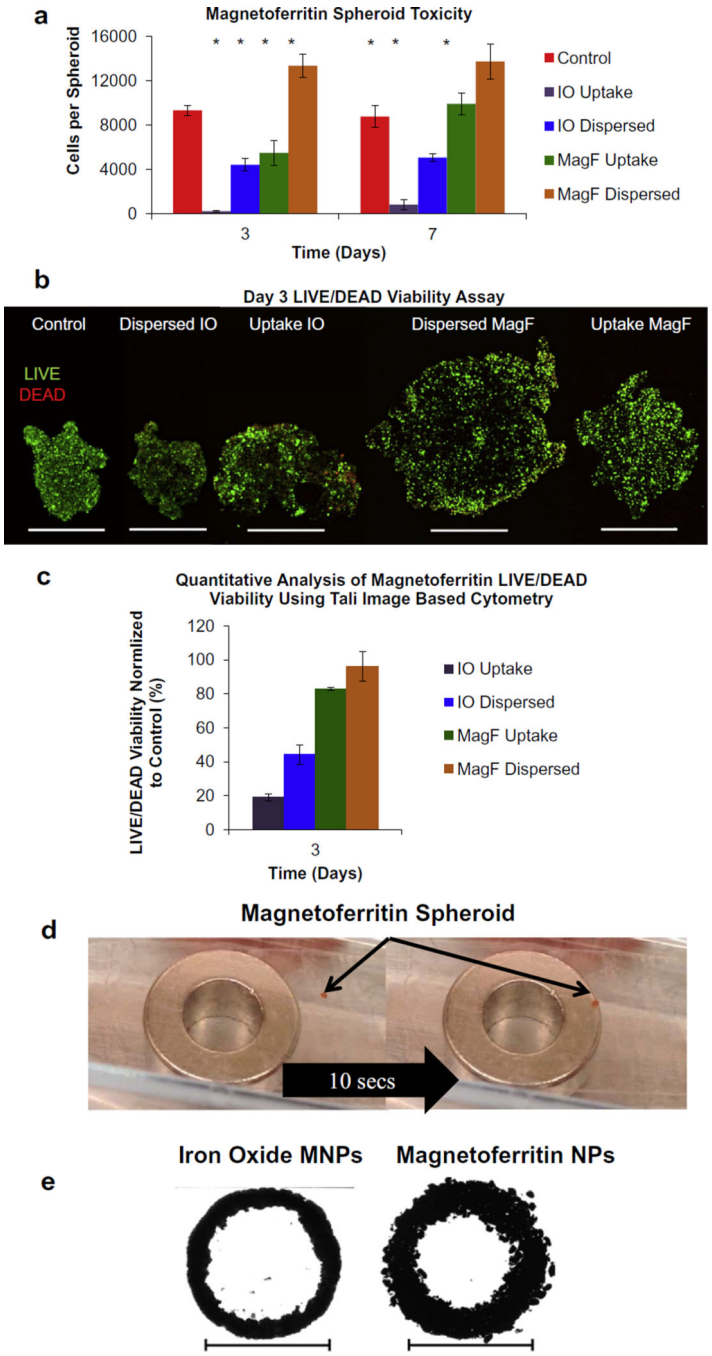

Fig. 4.

Magnetoferritin cellular spheroids for tissue engineering. (a) PrestoBlue viability assays were performed to compare cellular spheroids containing magnetoferritin NPs (MagF) and iron oxide MNPs (IO) to control spheroids without MNPs. Results confirmed that magnetoferritin NP spheroids maintained a high level of viability up to 1 week compared to control spheroids without MNPs and iron oxide MNPs spheroids (*$p < 0.05$). (b) Confocal microscopy was performed to confirm the effect of magnetic NPs on spheroid viability. Intact spheroids were analyzed on day 3 using magnetoferritin NPs (MagF) and iron oxide

MNPs (IO) and compared to MNP-free controls. Results showed that magnetoferritin NPs had no adverse effects on cells, confirmed by the low level of expression of dead (red) cells while spheroids containing iron oxide MNPs showed a high expression of dead cells (scale bar = 500 μm). The larger size of spheroids with magnetoferritin NPs can be attributed to the larger concentration of MNPs used (500 μg ml^{-1}), when compared to iron oxide MNP spheroids (300 μg ml^{-1}). (c) Finally, dissociated spheroid samples for each type were analyzed using cytometry with a LIVE/DEAD stain. Viability was quantified using a Tali Image-Based Cytometer (Green + Red System Protocol) and normalized to control spheroids without MNPs (control). Results showed that magnetoferritin NPs (MagF) expressed 83% and 96% viability for uptake and dispersed, respectively, while iron oxide MNPs (IO) demonstrated 19% and 44% viability for uptake and dispersed, respectively. (d) The ability of magnetoferritin cellular spheroids to magnetically attract to a permanent magnet was confirmed (magnet diameter = 10 mm). (e) Using magnetic force assembly, results showed a fused homogeneous tissue, with magnetoferritin serving as a comparable alternative to iron oxide magnetic MNPs for patterning and fusion. Scale bar = 10 mm.